

## Article

# Geopolymers Based on a Mixture of Steel Slag and Fly Ash, Activated with Rice Husks and Reinforced with *Guadua angustifolia* Fibers

William Aperador <sup>1</sup>, Jorge Bautista-Ruiz <sup>2,\*</sup> and Jorge Sánchez-Molina <sup>2</sup>

<sup>1</sup> School of Engineering, Universidad Militar Nueva Granada, Bogotá 110111, Colombia; william.aperador@unimilitar.edu.co

<sup>2</sup> Centro de Investigación de Materiales Cerámicos, Universidad Francisco de Paula Santander, San José de Cúcuta 540003, Colombia; jorgesm@ufps.edu.co

\* Correspondence: jorgebautista@ufps.edu.co

**Abstract:** At present, the conservation of the environment represents an objective that everyone wants to achieve. The construction industry has influenced the advancement of alternative materials that comply with sustainable development. In this article, reinforced concrete was obtained by mixing 80% blast furnace slag and 20% fly ash. These concentrations were chosen because they provide the lowest porosity in the cementitious matrix. Rice husk ash was used as an activator. *Guadua angustifolia* fibers were used to evaluate the mechanical performance of the concrete. The composition of the raw material was determined by X-ray fluorescence, the microstructure of the fibers by AFM, and the SEM technique was used to determine the surface characteristics of guadua fibers and concrete mixes. The structural characterization using XRD, the structure of the molecules of the guadua fiber, and the composition of the mixture's molecular mixtures were determined by FTIR spectroscopy. Its properties, such as tensile strength and flexural strength, were analyzed. The results indicated that the concrete with the addition of *Guadua angustifolia* fibers. The results indicated that the concrete with the addition of *guadua angustifolia* fibers showed the best mechanical behavior. Tensile strength was optimized, establishing values of 2.68 MPa for unreinforced concrete and up to 3.12 MPa for fiber-reinforced concrete. The flexural strength values increase at ages after 28 days due to the pozzolanic reaction generated. Values of 2.8 MPa were obtained for concrete without fiber and 3.5 MPa for concrete reinforced with *guadua angustifolia* fiber.

**Keywords:** guadua; slag; rice husk; fly ash; microstructure; tensile; flexural



**Citation:** Aperador, W.; Bautista-Ruiz, J.; Sánchez-Molina, J. Geopolymers Based on a Mixture of Steel Slag and Fly Ash, Activated with Rice Husks and Reinforced with *Guadua angustifolia* Fibers. *Sustainability* **2023**, *15*, 12404. <https://doi.org/10.3390/su151612404>

Academic Editors: John Vakros, Evroula Hapeshi, Catia Cannilla, Giuseppe Bonura and George Z. Kyzas

Received: 27 June 2023

Revised: 9 August 2023

Accepted: 12 August 2023

Published: 15 August 2023



**Copyright:** © 2023 by the authors. Licensee MDPI, Basel, Switzerland. This article is an open access article distributed under the terms and conditions of the Creative Commons Attribution (CC BY) license (<https://creativecommons.org/licenses/by/4.0/>).

## 1. Introduction

Concrete is the most used material in construction due to its physical-mechanical properties. It has excellent compressive strength but deficient tensile strength [1]. Reinforced concrete is used in structures subjected to tensile and bending efforts, generally with steel rods [2]. These reinforcements improve the system's behavior under tensile stresses, reducing the susceptibility to failure when the structures are exposed to the action of winds, thermal cycles, and traffic [3]. However, when steel is exposed to corrosive environments, a bond between steel and concrete is lost. Bond failure affects the structure's integrity due to the reduction of the cross-sectional area of the steel [2]. To improve the resistance in concrete, adding artificial and natural polymeric fibers has been proposed. The most significant environmental problem in Portland-type concrete is related to high CO<sub>2</sub> emissions [4]. Developing low-energy consumption ecological constructions with good resistance and durability has been proposed to counteract this situation [5]. Therefore, in the last two decades, research has been carried out on the production of geopolymers using by-products from industrial sectors such as steel, thermoelectric, and rice production [6].

The most common cement alternatives include fly ash (FA), ground granulated blast furnace slag (GGBFS), and silica fume (SF). Fly ash is a by-product of coal-fired electric power stations. There are two general classes of FA: Low-calcium fly ash (ASTM C618 [7] Class F, CaO < 10%) and high-calcium fly ash (ASTM C618 [7] Class C, CaO > 10%). The low-calcium FA is considered a normal pozzolan, consisting of silicon oxide and aluminum oxide, and to a lesser extent, by iron oxide. This type of FA requires calcium hydroxide (Ca(OH)<sub>2</sub>) because it has pozzolanic properties, and its particles need the presence of Potlandite, produced during clinker hydration, to react [8]. The addition of fly ash leads to lower heat of hydration, improves durability, and increases concrete strength by pozzolanic and filler effects at long ages [9]. Ground granulated blast furnace slag is a waste product from the iron manufacturing industry. The main components of GGBFS are CaO (30–35%), SiO<sub>2</sub> (28–38%), Al<sub>2</sub>O<sub>3</sub> (8–24%), and Mg (1–18%). The slag has hydraulic properties. Therefore, it would start to react since the setting moment. The slag's presence reduces the hydration heat and leads to an essential refinement of mortars and concrete microstructure [10]. Therefore, adding FA and GGBFS reduces the permeability of concrete and improves its resistance to aggressive environments [9].

The development of binary, ternary, and quaternary blended concretes, depending on the number of additions and their combinations used as partial replacement materials, is taking place to meet the requirements of strength and durability demanded by concrete technology. The utilization of fly ash and blast furnace slag provides an interesting alternative. Some researchers have carried out using the combination of these two by-products with Portland cement in the last decades. Shenchun Xu et al. [11] observed that increasing GGBFS (from 30% to 50%) while the content of FA was kept at 10% implied a reduction of compressive strength of about 14% at 28 days. An increase of FA amount (from 10% to 20%) while the content of GGBFS was 30% also reduced the compressive by about 12% at the same age. The sample with 30% slag and 10% fly ash presented the highest compressive strength, surpassing even those of the reference cement. The durability properties of the ternary concrete, containing fly ash and blast furnace slag, were also evaluated by immersion into 2% H<sub>2</sub>SO<sub>4</sub> solution for one year. The ternary concrete (25% FA and 15% GGBFS) was superior against sulfate attack, with minor weight loss and a slower decreasing rate of compressive strength [12]. Fernandez et al. [13] studied the influence of these two by-products on the physical and mechanical properties of ternary binders using two different types of cement. The initial heat of the hydration and the setting time was significantly reduced and delayed in the Portland cement with high alkali and high C3A content. In contrast, they were slightly delayed both in the Portland cement with low alkali and low C3A content.

The new engineering materials seek to satisfy mechanical, design, and cost requirements, reducing their environmental impact in the production or service phases. Worldwide, the growth of the construction industry has set itself the goal of supplying increasingly economical and environmentally friendly materials [14]. The development of alternative materials for producing cement and concretes has improved mechanical performance and durability, with results superior to those established for traditional concretes [15]. Concerning durability, natural fibers have been implemented due to their ease of obtaining and low contamination rate for other types of fibers currently used [4]. Specifically, some studies have focused on using guadua fibers due to their excellent physical-mechanical properties.

Research has allowed the development of new materials that are more resistant, durable, environmentally friendly, and suitable for the needs of the construction industry, with characteristics very similar to cement [16]. Consequently, most of the studies in the area of materials have focused on the replacement or modification of traditional cement [17]. Additionally, it has been proposed to reduce the carbon footprint by using waste from the iron and steel, thermoelectric, and rice processing industries. Specifically, blast furnace slags are combinations of clayey materials from iron ore and the chemical reaction between coke and sulfur [18]. The fly ashes produced in thermoelectric plants are considered polluting due to their very little use [19]. Another material from controlled combustion processes is

agro-industrial waste, such as rice husk ash [20]. Additionally, adding *Guadua angustifolia* fibers to the cement will allow its potential use in construction [5].

This study obtained reinforced concrete with mixtures of 80% steel slag and 20% fly ash. In previous works, it was shown that these concentrations reduce the porosity in the cementitious matrix. Rice husk ash was also used as an activator. *Guadua angustifolia* fibers were added to the cementitious matrix to determine the flexural properties. The research objective was to compare the mechanical performance of reinforced concrete with concrete samples without reinforcement.

## 2. Materials and Methods

### 2.1. Materials

Activated granulated blast furnace slag (BFS) was used as a cementing agent. It comes from the steel industry Acerías Paz del Río S.A., located in Boyacá–Colombia, dedicated to producing steel from iron ore, coke, and limestone. Class F fly ash (FA) was obtained from the Termopaipa thermoelectric plant and produced during coal combustion and gasification. The ashes are spherical particles (Figure 1) composed mainly of  $\text{SiO}_2$  and  $\text{Al}_2\text{O}_3$ , and to a lesser extent by oxides of Ca, Fe, and S. Likewise, rice husk ash (RHA) obtained through heat treatment of rice husks in a combustion furnace was used. The raw materials were characterized using a Malvern Panalytical X-ray fluorescence kit, reference Epsilon. The composition of the raw materials is reported in Figure 2.

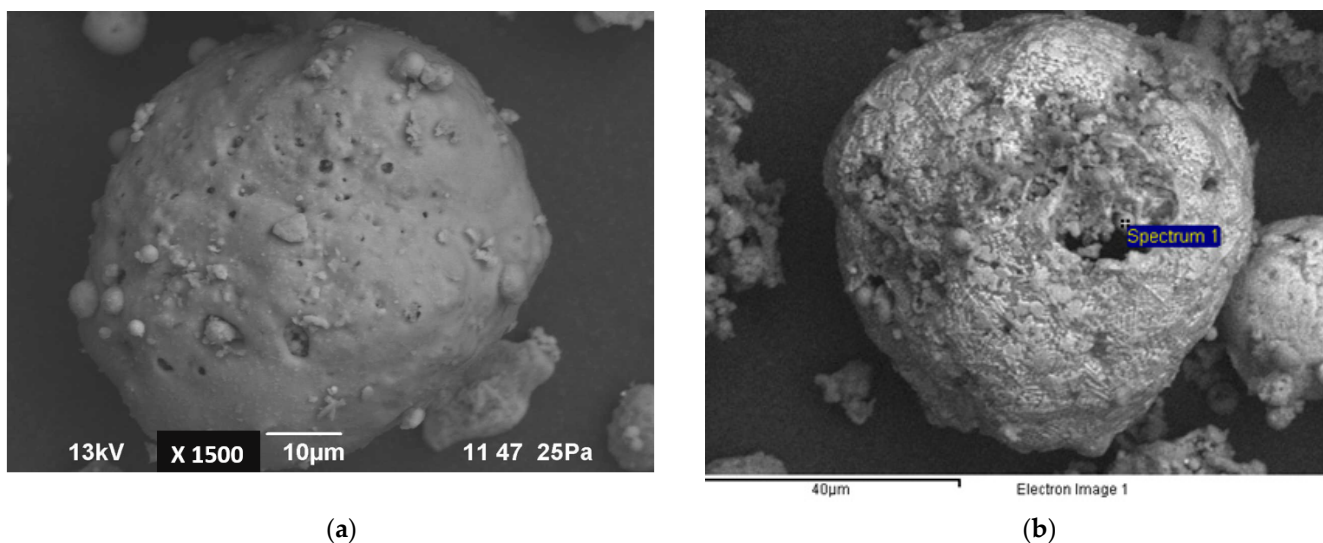


**Figure 1.** SEM micrograph of fly ash. (a) Morphology, and (b) chemical composition zone.

Table 1 shows the composition of the mixtures of blast furnace slag BFS and fly ash (FA) prepared in this research.

**Table 1.** Composition of blast furnace slag (BFS) mixtures and fly ash (FA).

Sample	Binder Material
Raw fiber	80% BFS, 20% FA
The embedded fiber in concrete	80% BFS, 20% and <i>Guadua angustifolia</i> fibers

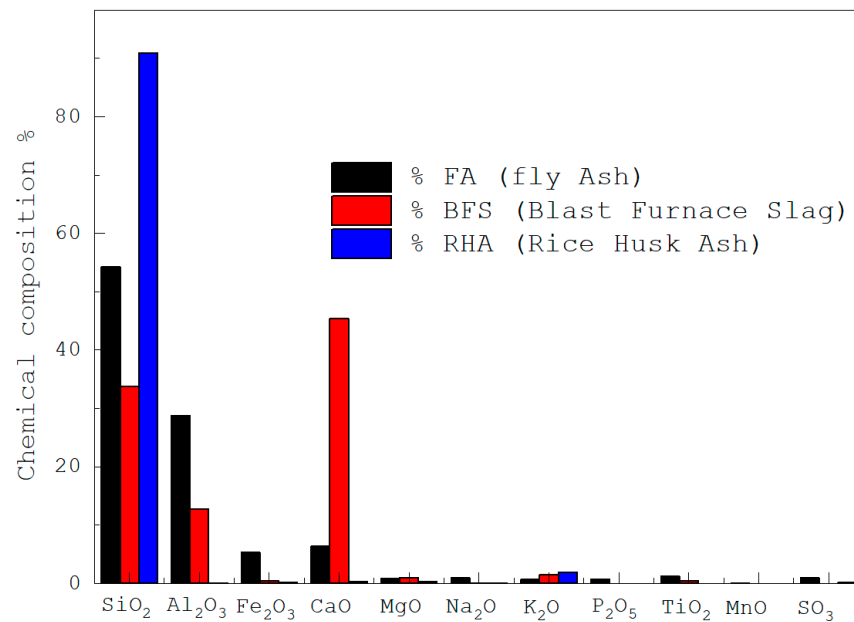


**Figure 2.** Chemical composition of blast furnace slag (BFS), fly ash (FA), and rice husk ash (RHA).

### 2.2. Alkali Activation of the Mixtures

Concrete mixes were manufactured using class F fly ash and blast furnace slag weight in different concentrations. The mixtures were activated by combining sodium hydroxide and rice husk ash/sodium silicate. This combination of activators was assigned based on the studies by Criado et al. [21]. The concretes' liquid/solid (L/S) ratios were calculated based on the mixing proportions and the chemical composition of the raw materials and activators. The proportions of the mixtures were 80% steel slag and 20% fly ash and subsequently activated by the combination of 85% NaOH 14M and 15% rice husk ash/sodium silicate [22]. The *Guadua angustifolia* fibers were added manually together with the aggregates in a percentage of 3% for the total weight of the mixture [23].

The sodium hydroxide/rice hull ash activating solutions were premixed and stored at room temperature and humid conditions for 24 h before use. For the manufacture of concrete, the aggregates and cementing materials were incorporated into a mixing pot for five minutes. Subsequently, the corresponding amounts of activating liquid were added to the dry materials, mixing at 22 rpm for five minutes. Each mixture in its fresh state was poured into molds, tamped, and compacted following the procedures described in the ASTM-C-109M standard [24]. After 24 h, the specimens were unmolded to undergo the curing process at 85 °C for another 24 h. Finally, the specimens were stored at room temperature.

### 2.3. Techniques

The ASTM C33 [25] standard determined the proportions of fine and coarse aggregates and the sizes of aggregates used in concrete mixes. *Guadua angustifolia* fibers and concrete mixes were characterized by Fourier Transform Infrared Spectroscopy (FTIR). A thermal analyzer was coupled to an FTIR spectrometer (IS20, Thermo Fisher Scientific Co.). The data acquisition frequency for FTIR spectrometry was 5 s, range of 400 cm<sup>-1</sup>–4000 cm<sup>-1</sup>, and spectral resolution of 1 cm<sup>-1</sup>. The crystalline character was determined by X-ray diffraction (XRD) using a PANalytical XPert PRO MRD instrument. This equipment has a copper tube ( $k = 1.54060 \text{ \AA}$ ), a goniometer with standard geometry resolution ( $\theta$ – $2\theta$ ), a minimum step size of 0.002, and a proportional X-ray counter.

Additionally, the *Guadua angustifolia* was determined by scanning electron microscopy (JEOL equipment) in backscattered electron mode (15 keV) and atomic force microscopy (AFM) in a Nanosurf Flex equipment configured in contact mode to determine the roughness values additionally. The fiber preparation process was carried out manually, guaranteeing that any chemical or biological agent did not alter the fibers. The fibers were cut to 3

and 0.034 cm in diameter, guaranteeing better workability and adherence to the rest of the mixture.

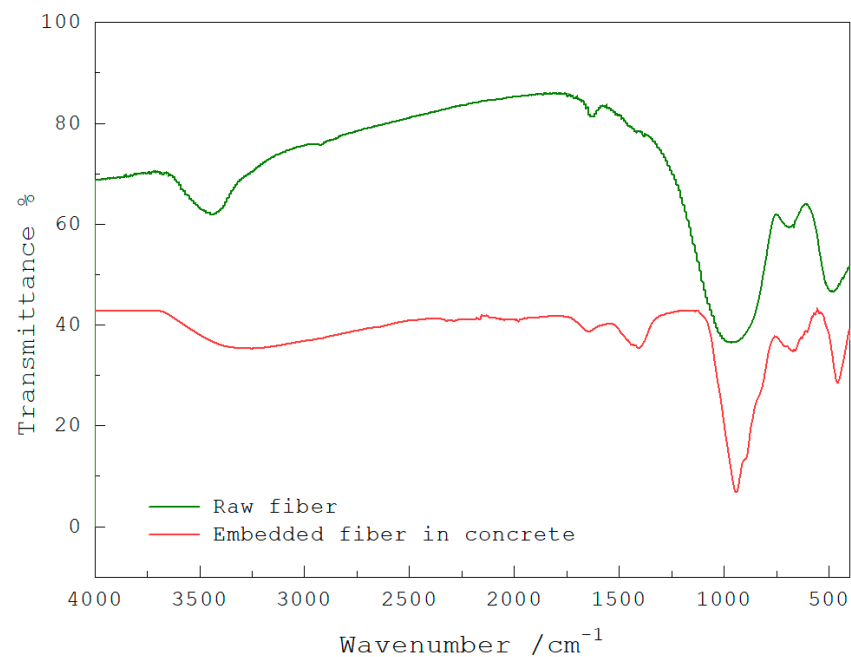
#### 2.4. Tensile Strength and Flexural Testing

The tensile strength was determined at the age of 28 and 90 days using the tensile splitting method for specimens with dimensions of  $15 \times 30$  cm in cylinders, according to the recommendations of ASTM-C-496 [26]. The load was applied by a hydraulic press controlled by an automated system until failure, and the load's application speed was 1290 N/s. In addition, prismatic specimens with dimensions of  $150 \times 150 \times 600$  mm were tested by bending at 90 days following the procedure of ASTM-C-78 [27]. The load was applied using a servo-controlled load frame with a maximum capacity of 100 kN. The load rate was 130 N/s and consisted of applying two continuous point loads without impacting the specimen's central third or middle third span.

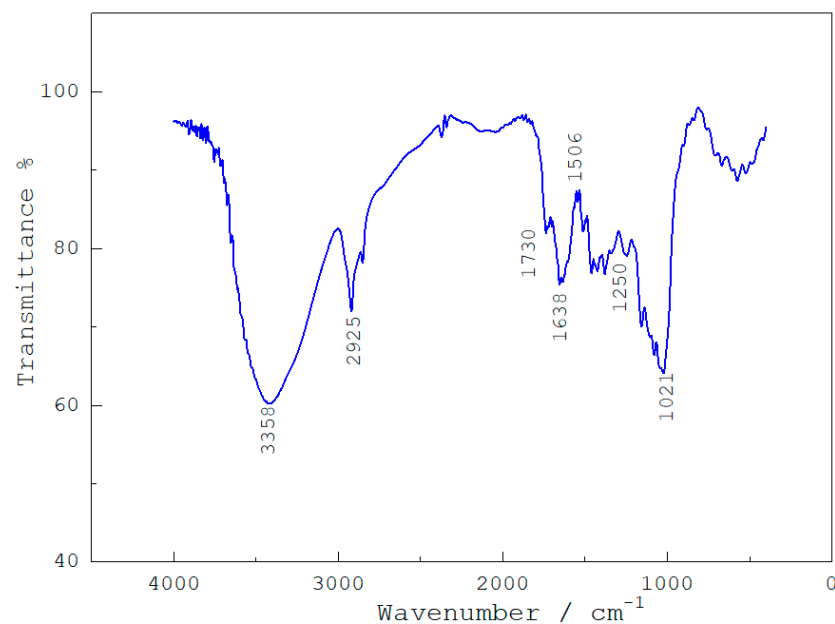
### 3. Results and Discussion

Figure 3 shows the results of the FTIR analysis of the *Guadua angustifolia* fibers. After the immersion treatment in  $\text{Ca}(\text{OH})_2$ , 3 Molar for 24 h, the functional groups present in the fibers were identified. The objective of the treatment was to eliminate biological and chemical agents that affected the quality of the concrete mixtures. The spectra (Figure 3) show a peak at  $1021 \text{ cm}^{-1}$ , corresponding to the modification of the chemical bonds related to the C–O group, indicating the existence of an amorphous phase [28]. The properties related to low molecular weight polysaccharide compounds are characterized by the asymmetric axial deformation of the C–O–C group according to the peak at  $1250 \text{ cm}^{-1}$ , which would confirm, in turn, the loss of lignin [29]. In general, the FTIR analysis established that the chemically treated *Guadua angustifolia* samples exhibited bands referring to crystalline cellulose. Modifications were also observed in the bands corresponding to hemicellulose and lignin components, indicating the elimination of these substances or the modification of their chemical bonds. The results infer the decrease in moisture absorption on the specimens. The bands at  $1250$  and  $1506 \text{ cm}^{-1}$  indicate a lower water absorption capacity and an increase in the crystalline phase. The peak at  $1638 \text{ cm}^{-1}$  is due to the modification of the cellulose phases. The peak at  $1730 \text{ cm}^{-1}$  is attributed to the carbonyl groups (C=O) of cetyl-esters of hemicellulose. Due to the alkaline treatment with  $\text{Ca}(\text{OH})_2$  on the lignocellulosic material, the peak has low intensity, and it is possible to relate this behavior to the conformation of amorphous material [30]. The band at  $3358 \text{ cm}^{-1}$  is due to the stretching of the –OH group, associated with the modification of the –OH bond of the cellulose molecule caused by the reactions with the  $\text{Ca}(\text{OH})_2$  solution. These last two bands indicate the presence of aldehydes that make up the solutions used during infiltration.

Figure 4 shows the concrete's FTIR spectrum without adding *Guadua angustifolia* fibers. In the zone from  $400$  to  $900 \text{ cm}^{-1}$ , small peaks are evident that confirm the formation of a geopolymer network between Si and Al, linked by oxygen bridges due to hydration processes. A band at  $1021 \text{ cm}^{-1}$  is related to the partial replacement of silicon by aluminum due to the composition of the steel slag and its addition to the mixture (80% by weight) [31]. The peak with the lowest intensity is related to the formation of the weak Al–O bond due to the dissolution of the precursor during geopolymerization and its subsequent reincorporation into the network, modifying the chemical environment of the bond. The band corresponding to the vibration at  $1506 \text{ cm}^{-1}$  is related to the carbonyl group's bonding due to the slag's CaO concentration [32]. This factor can be correlated with the mechanical properties of the concrete. The bands at  $1638$  and  $1730 \text{ cm}^{-1}$  are attributed to the reaction of  $\text{SiO}_4^{-2}$  in the C–S–H bonds in the hydration of the concrete [33]. The peak at  $2925 \text{ cm}^{-1}$  indicates the presence of water and sodium hydroxide. The peak displacement below  $3000 \text{ cm}^{-1}$  is due to high concentrations of the alkaline activator. The peak at  $3358 \text{ cm}^{-1}$  corresponds to the reaction of the activator with the calcium sulfate present in the mixture.



**Figure 3.** FTIR spectrum of *Guadua angustifolia* fibers.



**Figure 4.** FTIR spectrum of concrete samples with added fly ash and steel slag, activated by rice husk ash.

Figure 5 shows, by scanning electron microscopy, the morphology of the *Guadua angustifolia* fibers, a concrete sample without reinforcement, and a concrete sample reinforced with *Guadua angustifolia* fiber [34]. Figure 5a reveals details of the guadua fibers instead of sheets. Figure 4b is the detailed view (Figure 5a) of the surface of the *Guadua angustifolia* fibers. A rough surface and stretching are observed, forming undulations at the edges and minor fractures, indicating moderate fiber fragility [35]. Figure 5c shows the morphological characterization of the concrete mix without fiber reinforcement. In this micrograph, particles with various granulometry and irregular shapes are identified due to chemical reactivity and the action of surface tension forces during mixing to minimize free energy.

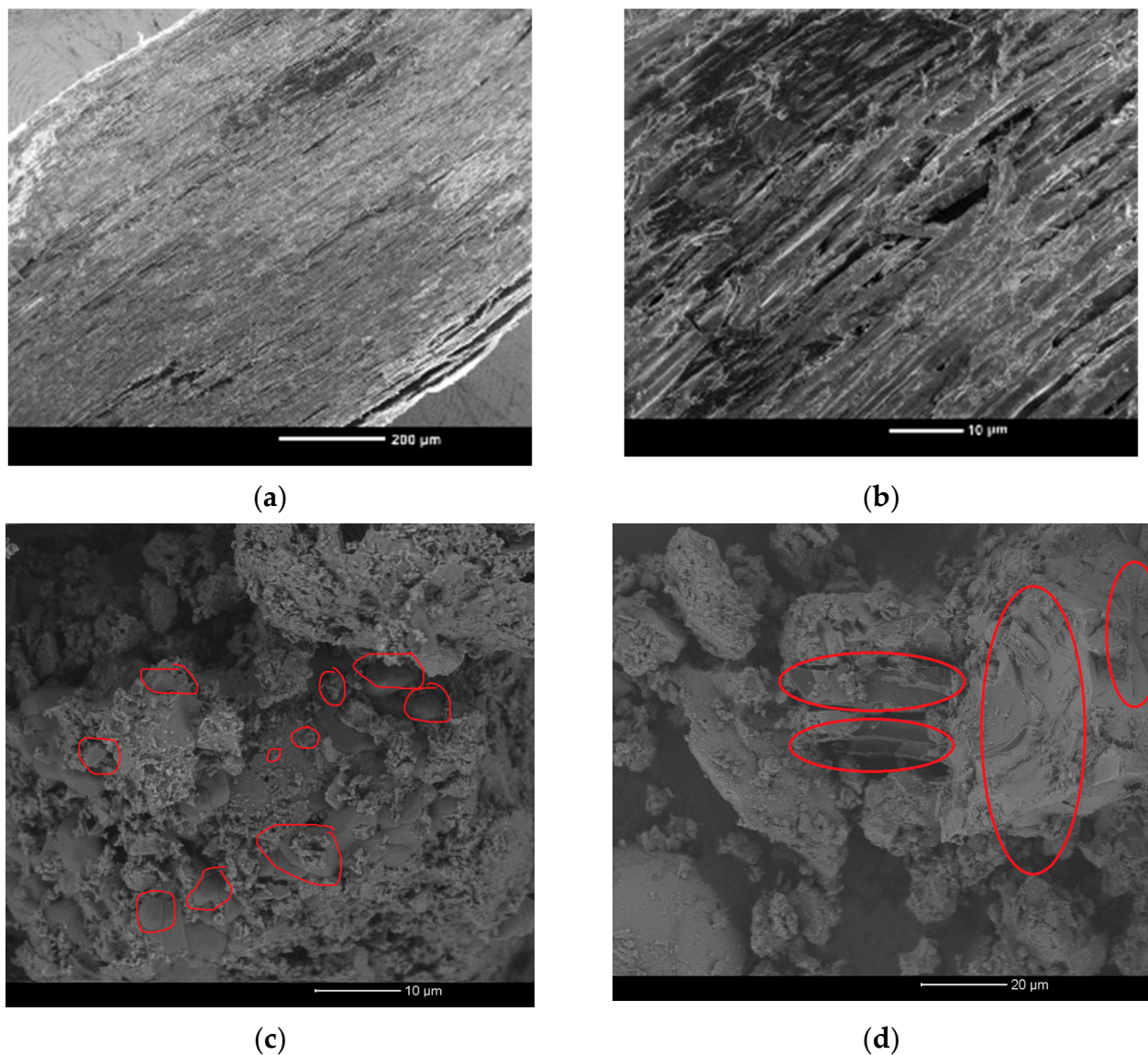


**Figure 5.** SEM micrographs. (a,b) *Guadua angustifolia* fiber, (c) concrete mix without guadua fiber reinforcement, and (d) concrete mix with guadua fiber reinforcement.

Additionally, two zones are observed, one compact and another region with very porous intergranular spacing related to the alkaline activation generated by rice husk ash. In Figure 5d, the morphology of the concrete samples is observed as a combined result of the contraction and expansion forces due to the interaction of the *Guadua angustifolia* fibers [36]. The different morphologies are more explicit in this micrograph Figure 5d because the hydrated products and sheet forms are more clearly revealed.

The characterization of the *Guadua angustifolia* fibers by AFM is shown in Figure 6. The analysis consisted of evaluating a section of  $35.8 \times 35.8 \mu\text{m}$  and determining the changes in the surface morphology of the fibers [37]. The surface irregularity provides greater adherence between the ceramic matrices and the fibers. The roughness value was determined at  $2.7832 \mu\text{m}$ . AFM analysis of the concrete samples was not possible due to the high porosity of the material.

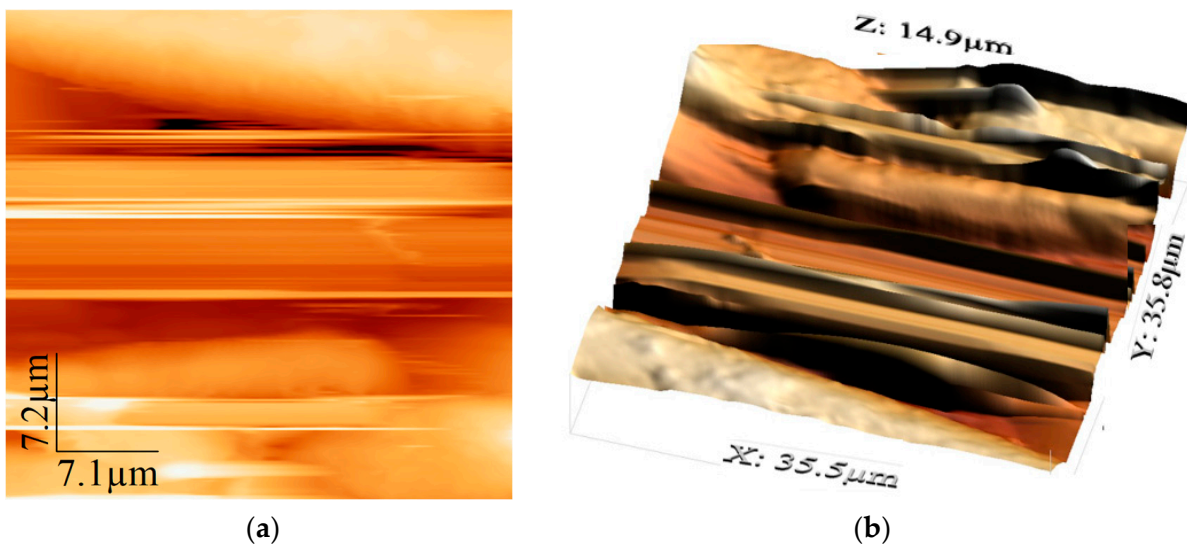


**Figure 6.** Morphology of *Guadua angustifolia* fibers obtained by AFM. (a) Two-dimensional, and (b) three-dimensional.

Figure 7 shows the diffractogram for the lignocellulosic samples analyzed by XRD. The samples show diffraction peaks related to the cellulosic fibers at position  $2\theta = 25.85^\circ$  corresponds to the crystallographic plane (002). The other peak, with less intensity, is at  $18.77^\circ$  relative to the crystallographic plane (101) [38]. These two peaks are related to the bands exhibited by the cellulose, indicating a high concentration of cellulose in the *Guadua angustifolia* fibers. Therefore, the XRD analyses allow us to infer that the chemical treatments lead to obtaining amorphous material, according to the intensity of the characteristic peak of the grid plane (002) and the depression in the peak at  $18.77^\circ$ .

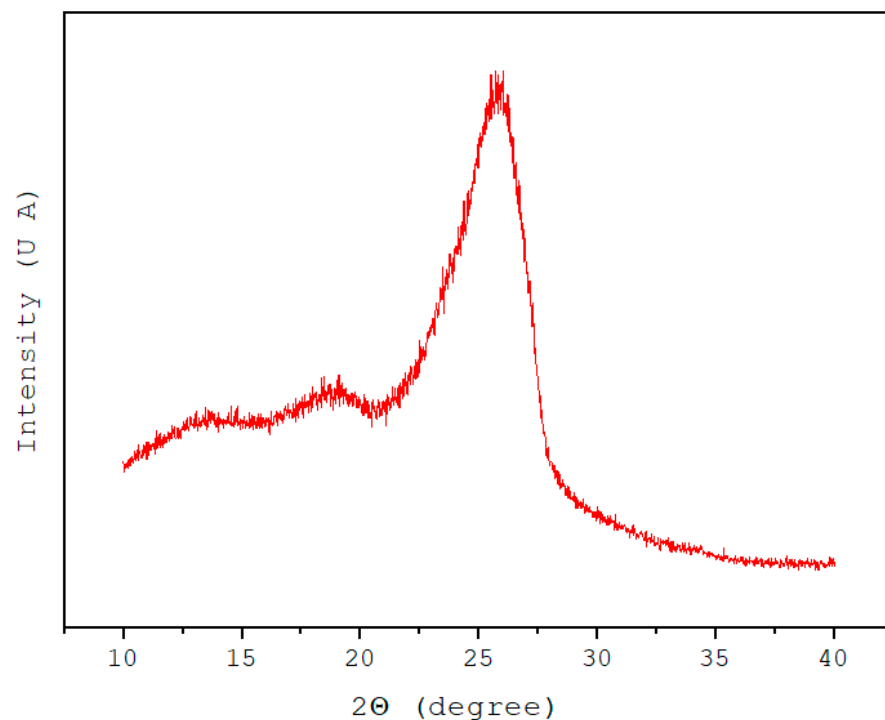


**Figure 7.** X-ray diffraction spectrum for *Guadua angustifolia* fibers.

The X-ray diffraction spectrum for the concrete samples with fibers is shown in Figure 8. The study established abundant glassy phases in the cementitious mix due to the high

percentages of fly ash and steel slag aggregation [39]. The identification of the phases was carried out from the interatomic distribution densities. The spectrum determined that the steel slag comprises a significant percentage of calcium silicate hydrates C-S-H, evidenced by a high-intensity peak centered around an angle ( $2\theta$ ) of  $32.2^\circ$ . Other peaks indicating the presence of C-S-H are found at positions of  $29.9^\circ$ ,  $50.7^\circ$ , and  $69.7^\circ$ . In addition, amorphous zones are evident in the silica gel's  $20^\circ$  to  $25^\circ$  indicator. The other compound corresponds to Calcium aluminosilicate, which is mixed with crystals of calcium oxide, aluminum oxide, and silicon oxide, its chemical formula  $\text{Al}_2\text{CaO}_8\text{Si}_2$  (JCPDS 00-034-1236) corresponding to positions  $27.87^\circ$ ,  $36.83^\circ$ ,  $42.32^\circ$ , and  $48, 16^\circ$  [40]. In this compound ( $\text{Al}_2\text{CaO}_8\text{Si}_2$ ), some or all free oxygen ions are replaced by other anions within the range kept in a Ca and Si crystal and a cell structure formed by the AlO type compound. Electrons replace the oxygen in the cells through treatment. Another compound is Tridymite ( $66.93^\circ$ ,  $82.57^\circ$ ), also known as Silicon Oxide ( $\text{SiO}_2$ ), stabilized with an alkali metal corresponding to an inorganic mineral with a Monoclinic crystalline system [41]. Tridymite is obtained at temperatures of  $1100^\circ\text{C}$ . Another mineral, but with minimal percentages in the mix, is the alumina-rich mullite with  $\text{Al}_6\text{Si}_2\text{O}_{12}$  (JCPDS 00-033-1161) composition. Its large number of oxygens leads to the formation of tetra-clusters. Mullite is the mineralogical composition in the silicoaluminate fly ash and influences the pozzolanic reactivity of the mixture [42].

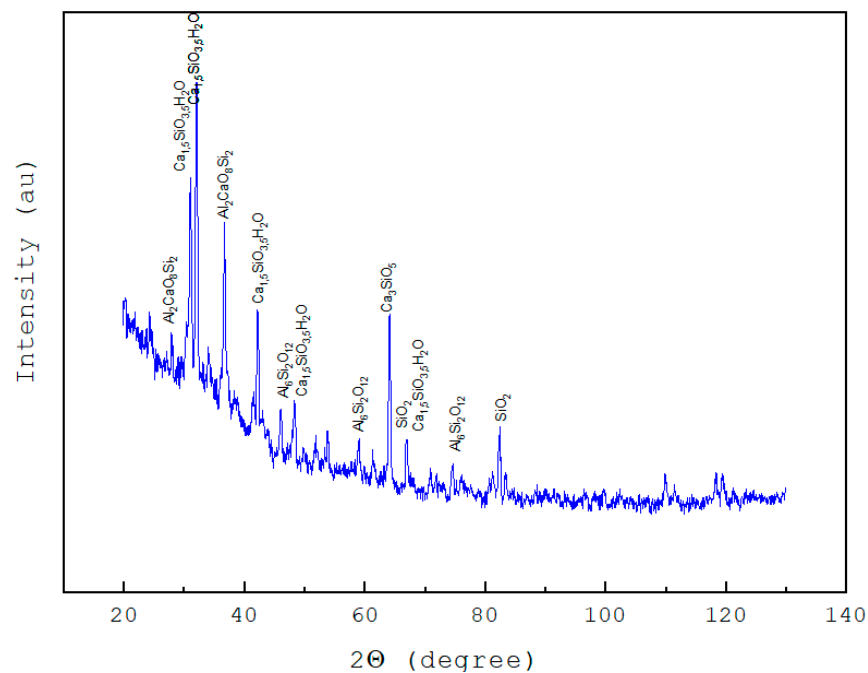


**Figure 8.** X-ray diffraction spectrum for the samples studied concrete with fibers.

Figure 9 shows the results obtained in the tensile strength tests. The concrete samples' highest tensile strength values were determined by mixing *Guadua angustifolia* fibers. After 28 days of curing, it was evident that concrete reinforced with guadua fibers increased resistance values by 28% compared to concrete without reinforcement [43]. Additionally, the study allowed increasing tensile strength at 90 days due to the incorporation of fly ash. At early ages, the fly ash fills the pores of the matrix. Therefore, at more prolonged periods of concrete evaluation, it was evident that the tensile strength values increased by 11% for mixtures with the addition of *Guadua angustifolia* fibers and 21% for mixtures without adding *Guadua angustifolia* fibers. This behavior is due to the slow pozzolanic reaction of the fly ash [29]. However, the slag hydrates more rapidly over time, improving tensile strength. The low reactivity values in concrete mixtures with the addition of fibers are due to the typical chemical reaction of the fibers concerning the other concrete components. It must be taken into account that reactions can occur, which can modify the total composition of the

mixture, forming expansions and alkalinity between the added materials. As mentioned, adding fly ash delays hydration due to 28.8% aluminate ions, as shown in Figure 9. Steel slag provides adequate flexural strength at early ages (28 days). However, at tiny grain sizes and in the presence of moisture, the concrete mix chemically reacts with rice husk ash to form cementitious compounds. A pozzolanic reaction can only occur over time with a ternary mixture of fly ash, steel slag, and rice husk ash. Therefore, this rapid reaction is due to the incorporation of steel slag in additions of 80%, as shown by the results of other investigations.

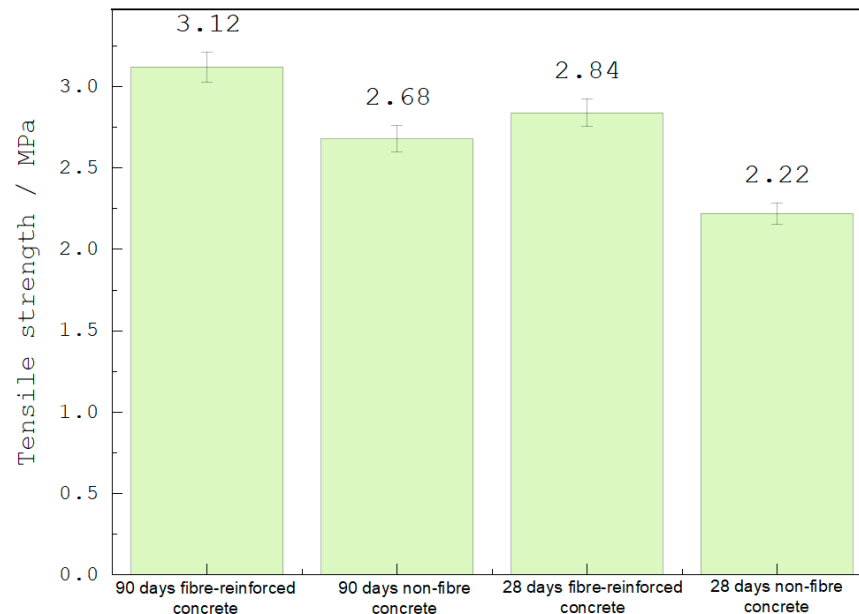


**Figure 9.** Variation of tensile strength values at 28 and 90 days in concrete mixes with and without adding *Guadua angustifolia* fibers.

Figure 10 lists the flexural strength values for the concrete samples with and without the addition of *Guadua angustifolia* fibers at times of 28 and 90 days [37]. The results show that the mixture with the addition of *Guadua angustifolia* fibers showed the highest values in flexural strength at 90 days. For mixtures without fiber reinforcement evaluated at 90 days, it was found that the flexural strength was 19% higher compared to the mixture evaluated at 28 days. In addition, the flexural strength results showed a 7% higher flexural strength than the mix evaluated at 28 days. In general, adding fly ash, steel slag, and activation with rice husk ash results in lower flexural strength as a function of time, and adding *Guadua angustifolia* fibers in the mix increases flexural strength. The flexural resistance values of the concrete mixtures added with *Guadua angustifolia* fibers were the highest, regardless of the curing time. These results are in agreement with the trends found in the analysis of tensile strength, where it has been shown that cementitious compounds typically gain less resistance due to the addition of *Guadua angustifolia* fibers [42,44]. The results here show that adding fibers affects the ternary mixtures more. This effect is related to the pozzolanic reaction over time. However, it has been observed that, at ages after 28 days, ternary mixed concretes have very little long-term strength because the effect of adding reinforcing fibers on flexural strength is high for early ages.

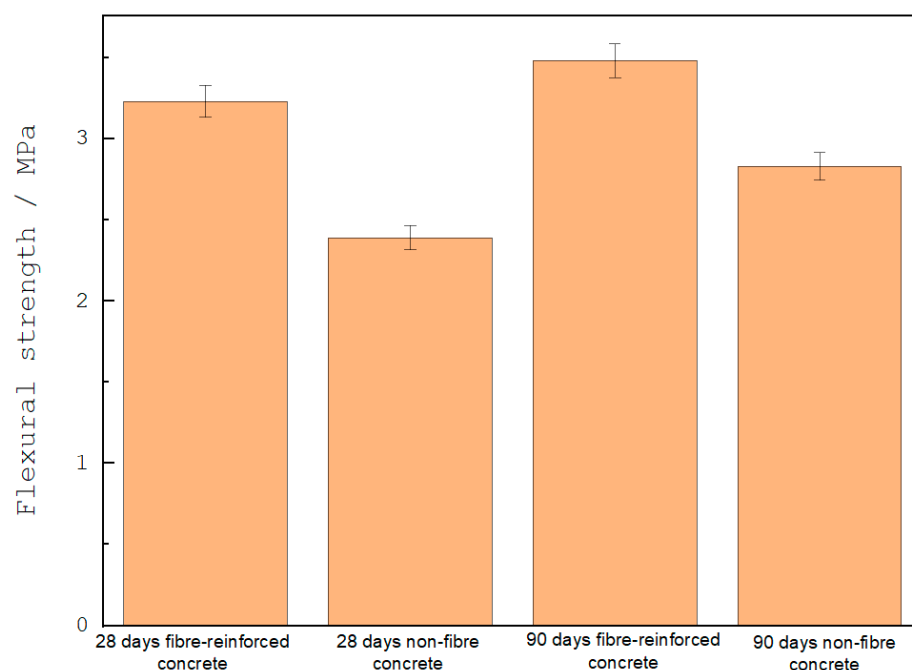


**Figure 10.** Variation of flexural strength values at 28 and 90 days in concrete mixes with and without adding *Guadua angustifolia* fibers.

#### 4. Conclusions

*Guadua angustifolia* is a renewable and sustainable material. Therefore, it is an attractive option from an environmental point of view. By incorporating guadua fibers into alkaline-activated concrete, the dependence on traditional construction materials, such as steel, which have a more significant environmental impact, can be reduced.

X-ray diffraction identified the presence of cellulose in the *Guadua angustifolia* fibers.

Employing X-ray diffraction, the hydration products were identified as calcium silicate gels, C-S-H (calcium silicate hydrate), and other crystalline compounds.

The mixture with additions of *Guadua angustifolia* fibers had the best mechanical behavior compared to the concrete without reinforcement. Incorporating guadua fibers into the ternary mixtures establishes the use of the mechanical properties of the *Guadua angustifolia* with the benefits of the materials that make up the alkaline-activated mixture. Tensile and flexural strength improve at ages older than 28 days due to the pozzolanic reaction attributed to the slag's hydraulic nature and the fly ash's slow pozzolanic reaction. FTIR determined these characteristics.

**Author Contributions:** Conceptualization, W.A. and J.B.-R.; methodology, J.S.-M.; software, W.A.; validation, J.B.-R.; formal analysis, J.S.-M.; investigation, W.A. and J.B.-R. All authors have read and agreed to the published version of the manuscript.

**Funding:** This research received no external funding.

**Institutional Review Board Statement:** Not applicable.

**Acknowledgments:** W. Aperador acknowledges the Universidad Militar Nueva Granada.

**Conflicts of Interest:** The authors declare no conflict of interest.

#### References

- De Sá, F.; Silva, F.; Cardoso, D. Tensile and flexural performance of concrete members reinforced with polypropylene fibers and GFRP bars. *Compos. Struct.* **2020**, *253*, 112784. [\[CrossRef\]](#)
- Okeil, A.; Matsumoto, K.; Nagai, K. Investigation on local bond behavior in concrete and cement paste around a deformed bar by using DIC technique. *Cem Concr Compos* **2020**, *109*, 103540. [\[CrossRef\]](#)

3. Li, Y.-F.; Hao, G.-W.; Syu, J.-Y.; Chen, B.-Y.; Lee, W.-H.; Tsai, Y.K. Use of Geopolymer and Carbon Fiber-Reinforced Polymer for Repairing Reinforced Concrete Deck Soffit. *Materials* **2023**, *16*, 4459. [[CrossRef](#)] [[PubMed](#)]
4. Ghavami, K. Bamboo as reinforcement in structural concrete elements. *Cem. Concr. Compos.* **2005**, *27*, 637–649. [[CrossRef](#)]
5. Drury, B.; Padfield, C.; Russo, M.; Swygart, L.; Spalton, O.; Froggatt, S.; Mofidi, A. Assessment of the Compression Properties of Different Giant Bamboo Species for Sustainable Construction. *Sustainability* **2023**, *15*, 6472. [[CrossRef](#)]
6. Usman-Kankia, M.; Baloo, L.; Danlami, N.; Zawawi, N.A.; Bello, A.; Muhammad, S.I. Microstructural Analysis and Compressive Strength of Fly Ash and Petroleum Sludge Ash Geopolymer Mortar under High Temperatures. *Sustainability* **2023**, *15*, 9846. [[CrossRef](#)]
7. ASTM C618-22; Standard Specification for Coal Fly Ash and Raw or Calcined Natural Pozzolan for Use in Concrete. ASTM International: West Conshohocken, PA, USA, 2023.
8. Garcia-Lodeiro, I.; Boudissa, N.; Fernandez-Jimenez, A.; Palomo, A. Use of clays in alkaline hybrid cement preparation. The role of bentonites. *Mater. Lett.* **2018**, *233*, 134–137. [[CrossRef](#)]
9. Huang, P.; Huang, B.; Li, J.; Wu, N.; Xu, Q. Application of sugar cane bagasse ash as filler in ultra-high-performance concrete. *J. Build. Eng.* **2023**, *71*, 106447. [[CrossRef](#)]
10. Yang, Z.; Xiong, X.; Chen, S.; Briseghella, B.; Marano, G.C.; Zhang, Y. Effect of fineness on the hydration and microstructure of cementitious materials with high-volume steel slag and blast furnace slag. *J. Build. Eng.* **2023**, *72*, 106682. [[CrossRef](#)]
11. Xu, S.; Yuan, P.; Liu, J.; Pan, Z.; Liu, Z.; Su, Y.; Li, J.; Wu, C. Development and preliminary mix design of ultra-high-performance concrete based on geopolymer. *Constr. Build Mater.* **2021**, *308*, 125110. [[CrossRef](#)]
12. Zeng, Q.; Liu, X.; Zhang, Z.; Wei, C.; Xu, C. Synergistic utilization of blast furnace slag with other industrial solid wastes in cement and concrete industry: Synergistic mechanisms, applications, and challenges. *Green Energy Environ.* **2023**, *1*, 100012. [[CrossRef](#)]
13. Fernandez, A.; Alonso, M.C.; García-Calvo, J.L.; Lothenbach, B. Influence of the synergy between mineral additions and Portland cement in the physical-mechanical properties of ternary binders. *Mater. de Construcción.* **2016**, *66*, 1–12. [[CrossRef](#)]
14. Zhou, A.; Wei, H.; Guo, H.; Zhang, W.; Liu, T.; Zou, D. Mechanical performance and environmental potential of concrete with engineering sediment waste for sustainable built environment. *Resour. Recycl.* **2023**, *189*, 106742. [[CrossRef](#)]
15. Afolalu, S.A.; Okwilagwe, O.; Emetere, M.M.; Ikumapayi, O.M. Impact and optimization of a new paradigm in engineering economics for sustainable manufacturing operations. *Mater. Today Proc.* **2021**, *44*, 2889–2894. [[CrossRef](#)]
16. Caicedo, J.C.; Ramirez-Malule, H.; Aperador, W. Mechanical properties evolution in carbon foams obtained from *Guadua angustifolia*. *Diam. Relat. Mater.* **2020**, *107*, 107901. [[CrossRef](#)]
17. Aperador, W.; Mejía de Gutiérrez, R.; Bastidas, D.M. Steel corrosion behaviour in carbonated alkali-activated slag concrete. *Corros. Sci.* **2009**, *51*, 2027–2033. [[CrossRef](#)]
18. Montoya, R.; Aperador, W.; Bastidas, D.M. Influence of conductivity on cathodic protection of reinforced alkali-activated slag mortar using the finite element method. *Corros. Sci.* **2009**, *51*, 2857–2862. [[CrossRef](#)]
19. Ziejewska, C.; Marczyk, J.; Korniejewski, K.; Bednarski, S.; Sroczek, P.; Łach, M.; Mikula, J.; Figiela, B.; Szechyńska-Hebda, M.; Hebda, M. 3D Printing of Concrete-Geopolymer Hybrids. *Materials* **2022**, *15*, 2819. [[CrossRef](#)]
20. Su, Q.; Xu, J. Mechanical properties of concrete containing glass sand and rice husk ash. *Constr. Build Mater.* **2023**, *393*, 132053. [[CrossRef](#)]
21. Criado, M.; Aperador, W.; Sobrados, I. Microstructural and Mechanical Properties of Alkali Activated Colombian Raw Materials. *Materials* **2016**, *9*, 158. [[CrossRef](#)]
22. Lilargem-Rocha, D.; Tambara, J.; Marvila, M.T.; Pereira, E.C.; Souza, D.; De Azevedo, A. A Review of the Use of Natural Fibers in Cement Composites: Concepts, Applications and Brazilian History. *Polymers* **2022**, *14*, 2043. [[CrossRef](#)] [[PubMed](#)]
23. ASTM C496-96; Standard Test Method for Splitting Tensile Strength of Cylindrical Concrete Specimens. ASTM International: West Conshohocken, PA, USA, 2017.
24. ASTM C109/C109M-20; Standard Test Method for Compressive Strength of Hydraulic Cement Mortars. ASTM International: West Conshohocken, PA, USA, 2020.
25. ASTM C33/C33M-18; Standard Specification for Concrete Aggregates. ASTM International: Philadelphia, PA, USA, 2003.
26. ASTM C496/C496M-17; Standard Test Method for Splitting Tensile Strength of Cylindrical Concrete Specimens. ASTM International: West Conshohocken, PA, USA, 2017.
27. ASTM C78-09; Standard Test Method for Flexural Strength of Concrete. ASTM International: West Conshohocken, PA, USA, 2010.
28. Sanchez-Echeverri, L.A.; Ganjian, E.; Medina-Perilla, J.A.; Quintana, G.C.; Sanchez-Toro, J.H.; Tyrer, M. Mechanical refining combined with chemical treatment for the processing of Bamboo fibers to produce efficient cement composites. *Constr. Build Mater.* **2021**, *269*, 121232. [[CrossRef](#)]
29. Bala, A.; Gupta, S. Engineered bamboo and bamboo-reinforced concrete elements as sustainable building materials: A review. *Constr. Build Mater.* **2023**, *394*, 132116. [[CrossRef](#)]
30. Kadivar, M.; Gauss, C.; Marmol, G.; De Sá, A.D.; Fioroni, C.; Ghavami, K.; Savastano, H. The influence of the initial moisture content on densification process of *D. asper* bamboo: Physical-chemical and bending characterization. *Constr. Build Mater.* **2019**, *229*, 116896. [[CrossRef](#)]
31. Libre, R.G.; Leañó, J.L.; Lopez, L.F.; Cacanando, C.J.; Promentilla, M.A.; Ongpeng, J.M. Microstructure and mechanical performance of bamboo fiber reinforced mill-scale—Fly-ash based geopolymer mortars. *Chem. Eng.* **2023**, *6*, 100110. [[CrossRef](#)]

32. Hughes, T.L.; Methven, C.M.; Jones, T.G.; Pelham, S.E.; Fletcher, P.; Hall, C. Determining cement composition by Fourier transform infrared spectroscopy. *Adv. Cem. Based Mater.* **1995**, *2*, 91–104. [[CrossRef](#)]
33. Mendes dos Santos, V.H.; Pontin, D.; Dias, G.G.; Guimarães, A.S.; Bordulis, R.M.; Kerber, M.K.; Oliveira, S.M.; Dalla, F. Application of Fourier Transform infrared spectroscopy (FTIR) coupled with multivariate regression for calcium carbonate (CaCO<sub>3</sub>) quantification in cement. *Constr. Build Mater.* **2021**, *313*, 125413. [[CrossRef](#)]
34. Uppal, N.; Pappu, A.; Sorna, V.; Thakur, K. Cellulosic fibres-based epoxy composites: From bioresources to a circular economy. *Ind. Crops Prod.* **2022**, *182*, 114895. [[CrossRef](#)]
35. Savastano, H.; Santos, S.F.; Fiorelli, J.; Agopyan, V. Sustainable use of vegetable fibres and particles in civil construction. In *Woodhead Publishing Series in Civil and Structural Engineering, Sustainability of Construction Materials*, 2nd ed.; Khatib, J.M., Ed.; Woodhead Publishing: Sawston, UK, 2016; pp. 477–520.
36. Perremans, D.; Trujillo, E.; Ivens, J.; Van Vuure, A.W. Effect of discontinuities in bamboo fibre reinforced epoxy composites. *Compos. Sci. Technol.* **2018**, *155*, 50–57. [[CrossRef](#)]
37. Fuentes, C.A.; Tran, L.Q.N.; Dupont-Gillain, C.; Vanderlinden, W.; De Feyter, S.; Van Vuure, A.W.; Verpoest, I. Wetting behaviour and surface properties of technical bamboo fibres. *Colloids Surf. A Physicochem. Eng. Asp.* **2011**, *380*, 89–99. [[CrossRef](#)]
38. Kelkar, B.U.; Shukla, S.R.; Yadav, S.M. Interlaminar fracture energy and its dependence on microstructure in three bamboo species of commercial importance. *Theor. Appl. Mech.* **2023**, *124*, 103824. [[CrossRef](#)]
39. Ishwarya, G.; Singh, B.; Deshwal, S.; Bhattacharyya, S.K. Effect of sodium carbonate/sodium silicate activator on the rheology, geopolymerization and strength of fly ash/slag geopolymer paste. *Cem. Concr. Compos.* **2019**, *97*, 226–238.
40. Chen, Z.; Lu, S.; Tang, M.; Ding, J.; Buekens, A.; Yang, J.; Qiu, Q.; Yan, J. Mechanical activation of fly ash from MSWI for utilization in cementitious materials. *Waste Manag.* **2019**, *88*, 182–190. [[CrossRef](#)]
41. Chen, S.; Zeng, W.; Gu, L.; Lin, W.; Wu, B.; Xue, K.; Hsu, H. Effects of combining binary mineral admixtures and manufactured basalt sand on the microscopic properties of mortar. *J. Build. Eng.* **2023**, *66*, 105873. [[CrossRef](#)]
42. Yingliang, Z.; Zhengyu, M.; Jingping, Q.; Xiaogang, S.; Xiaowei, G. Experimental study on the utilization of steel slag for cemented ultra-fine tailings backfill. *Powder Technol.* **2020**, *375*, 284–291. [[CrossRef](#)]
43. Chen, Z.; Ma, R.; Du, Y.; Wang, X. State-of-the-art review on research and application of original bamboo-based composite components in structural engineering. *Structures* **2022**, *35*, 1010–1029. [[CrossRef](#)]
44. Correal, J.F.; Calvo, A.F.; Trujillo, D.; Echeverry, J.S. Inference of mechanical properties and structural grades of bamboo by machine learning methods. *Constr. Build Mater.* **2022**, *354*, 129116. [[CrossRef](#)]

**Disclaimer/Publisher’s Note:** The statements, opinions and data contained in all publications are solely those of the individual author(s) and contributor(s) and not of MDPI and/or the editor(s). MDPI and/or the editor(s) disclaim responsibility for any injury to people or property resulting from any ideas, methods, instructions or products referred to in the content.